HHS Public Access

Author manuscript

Biochemistry. Author manuscript; available in PMC 2016 November 10.

Published in final edited form as:

Biochemistry. 2015 November 10; 54(44): 6704–6711. doi:10.1021/acs.biochem.5b00567.

Analysis of the Ability of Pramlintide to Inhibit Amyloid Formation by Human Islet Amyloid Polypeptide Reveals a Balance between Optimum Recognition and Reduced Amyloidgenicity

Hui Wang[(1)], **Zachary Ridgway**[(1)], **Ping Cao**[(1),(2)], **Bela Ruzsicska**[(3)], and **Daniel P. Raleigh**[(1),(3),(4),(5),*]

[(1)]Department of Chemistry, State University of New York at Stony Brook, Stony Brook, NY 11794-3400, USA

[(2)]Structural Biology Program, Kimmel Center for Biology and Medicine at the Skirball Institute, New York University School of Medicine, New York, NY, USA

[(3)]Institute for Chemical Biology and Drug Discovery, Stony Brook University, Stony Brook, NY 11794-3400, USA

[(4)]Graduate Program in Biochemistry and Structural Biology, Graduate program in Biophysics, Stony Brook University, Stony Brook, NY 11794-3400, USA

[(5)]Research Department of Structural and Molecular Biology, University College London, Gower Street London, WC1E 6BT, UK

Abstract

The hormone human islet amyloid polypeptide (hIAPP or amylin) plays a role in glucose metabolism, but forms amyloid in the pancreas in type 2 diabetes (T2D) and is associated with β-cell death and dysfunction in the disease. Inhibitors of islet amyloid have therapeutic potential, however there are no clinically approved inhibitors and the mode of action of existing inhibitors is not well understood. Rat IAPP (rIAPP), differs from hIAPP at six positions, does not form amyloid and is an inhibitor of amyloid formation by hIAPP. Five of the six differences are located within residues 20-29, and three of them are Pro residues, which are well known disruptors of β-sheet structure. rIAPP is thus a natural example of a "β-breaker inhibitor"; a molecule which combines a recognition element with an entity that inhibits β-sheet formation. Pramlintide (PM) is a peptide drug approved for use as an adjunct to insulin therapy for treatment of diabetes. PM was developed by introducing the three Pro substitutions found in rIAPP into hIAPP. Thus, it more closely resembles the human peptide than does rIAPP. Here we examine and compare the ability of rIAPP, PM and a set of designed analogs of hIAPP to inhibit amyloid formation by hIAPP, in

*Corresponding Author: D.P.R. Phone: 631-632-9547, Fax: 631-632-7960, Daniel.raleigh@stonybrook.edu.

Author Contributions: The manuscript was written through contributions of all authors. All authors have given approval to the final version of the manuscript.

Supporting Information Availible: TEM control studies of rIAPP and PM, a figure of Mass spec control studies of rIAPP, PM, and hIAPP, a figure showing the results of seeding studies, figures showing the effect of DM-IAPP on hIAPP amyloid formation, and TEM studies of DM-IAPP / hIAPP mixtures. The supporting information is available free of charge on the ACS publications website.

order to elucidate the factors which lead to effective peptide based inhibitors. Our results reveal, for this class of molecules, a balance between the reduced amyloidogenicity of the inhibitory sequence on the one hand and its ability to recognize hIAPP on the other.

Keywords

Amylin; Islet Amyloid Polypeptide; Pramlintide; Amyloid; Inhibitor; Type-2 Diabetes

Introduction

Amyloid formation plays a role in over 25 different human diseases including Alzheimer's disease, Parkinson's disease and type 2 diabetes (T2D).[1, 2] Islet amyloid polypeptide (IAPP or amylin) is a neuropancreatic hormone that plays a role in metabolism and energy homeostasis, but forms fibrillar amyloid deposits in the pancreatic islets of Langerhans in T2D by an unknown mechanism.[3, 4] The process of amyloid formation is associated with reduced β-cell mass, and is believed to contribute to T2D,[5-7] and to the failure of islet transplantation.[8, 9] There are no clinically approved inhibitors of islet amyloid formation, despite its importance and the mode of action of existing inhibitors is not well understood. Most of the work on IAPP inhibitors has focused on the effects of polyphenols or on polypeptide based inhibitors.[10-18] A popular approach for the design of inhibitors of amyloid formation relies on the concept of β-breaker inhibitors, in which a recognition element that targets the polypeptide of interest, is combined with a moiety that prevents the formation or propagation of β-sheet structure. Here we examine the ability of a set of rationally designed and clinically relevant mutants of human IAPP (hIAPP) to inhibit amyloid by wild type hIAPP. This study reveals that for this class of peptide based inhibitors, optimum design involves a balance between the ability to recognize hIAPP and the reduced amyloidogenicity of the inhibitory sequence.

Mature hIAPP is a 37 residue hormone with a disulfide bond between Cys-2 and Cys-7 and an amidated C-terminus (Figure 1). It aggressively forms amyloid *in vitro* and is toxic to cultured pancreatic islet β-cells and to islets.[19] Rat IAPP (rIAPP) differs from hIAPP at six positions, does not form amyloid, is not toxic and is a moderately effective inhibitor of hIAPP amyloid formation *in vitro*.[20] Five of the six differences relative to hIAPP are located in the region of residues 23-29, which is believed to be an important amyloidgenic segment.[21] rIAPP contains three prolines in this region (Pro-25, Pro-28 and Pro-29), which are well known disruptors of β-sheet structures. The other differences between rIAPP and hIAPP involve the replacement of His-18, Phe-23 and Ile-26 in hIAPP with Arg-18, Leu-23 and Val-26 in rIAPP respectively (Figure 1). Thus rIAPP can be thought of as a natural example of a β-breaker inhibitor. In this case, the first 22 residues and /or the C-terminal 7 residues act as recognition elements, while the segment containing the multiple proline residues acts as the β-breaker motif.

hIAPP complements insulin in maintaining glucose homeostasis by suppressing postprandial glucagon secretion, helping regulate gastric emptying and suppressing food intake.[22-26] hIAPP is thus an attractive adjunct to insulin therapy, however, hIAPP aggressively forms

toxic aggregates in solution, leading to difficulty in its formulation and storage. A soluble analog of hIAPP, pramlintide (PM), is approved by the FDA as an adjunct to insulin therapy for both type 1 diabetes and T2D. PM was designed by substituting the proline residues found in rIAPP into the human peptide to render it non-amyloidgenic, but to retain its activity (Figure 1).[27]

rIAPP has been proposed to inhibit hIAPP amyloid formation by binding to early, potentially partially helical intermediates, through the N-terminal half to two thirds of the peptide and then preventing propagation of intermolecular β-sheet structure.[20] Peptide mapping studies have provided evidence that important interactions between hIAPP monomers occur in this region, centered near residue 15, during the early stages of aggregation. This region may also be critical for hIAPP-rIAPP interactions as well, given the extremely high sequence identity from residues 1 through 22.[28] Structural studies indirectly support a helical model for initial steps of aggregation with helical structure localized between residues 8 to 22 and with inter peptide interactions in this region, although other experiments suggest different initial modes of oligomerization of hIAPP.[29-31] PM is expected to be a better inhibitor of hIAPP than rIAPP if recognition involves this region since hIAPP and PM are identical over the first 24 residues, and PM contains the same proline residues as rIAPP. Limited biophysical studies have been performed with PM. Nonoyama et al have reported that PM is disordered as a monomer and that its aggregation is sensitive to pH.[32] There are no reported studies of the potential inhibitory effects of PM on amyloid formation by hIAPP. Here, we compare the ability of PM and rIAPP as well as two mutants of PM, His18Arg pramlintide (H18R PM) and Phe23Leu pramlintide (F23L PM) to inhibit amyloid formation by the human peptide. The latter two mutations are chosen because they are the least conservative, non-proline substitutions between rIAPP and hIAPP. Our results provide clues to the optimization of peptide based hIAPP amyloid inhibitors, which should be useful for future rational inhibitor design.

Materials and Methods

Peptide Synthesis and Purification

All peptides were synthesized using a CEM microwave peptide synthesizer on a 0.25 mmol scale utilizing 9-fluornylmethoxycarbonyl (Fmoc) chemistry. Solvents used were ACS-grade. 5-(4′-Fmoc-aminomethyl-3′,5-dimethoxyphenol) valeric acid (PAL-PEG) resin was used to afford an amidated c-terminus. Fmoc-protected pseudoproline (oxazolidine) dipeptide derivatives were incorporated to improve the yield as previously described.[33] Standard Fmoc reaction cycles were used.[34] The first residue attached to the resin, all β-branched residues, all pseudoproline dipeptide derivatives and the residues directly following pseudoproline dipeptide derivatives were double-coupled. The peptides were cleaved from the resin through the use of standard trifluoroacetic acid (TFA) methods. After cleavage, the crude peptides were dissolved into 20% (v/v) acetic acid and then lyophilized. This was repeated several times prior to disulfide bond formation and purification to improve their solubility. The peptides were oxidized to form the disulfide bond using 100% dimethyl sulfoxide at room temperature and were purified via reverse-phase high-performance liquid chromatography (RP-HPLC) using a Vydac C18 preparative column.[35]

Analytical HPLC was used to check the purity of the peptides before each experiment. The masses of the pure peptides were confirmed by MALDI time-of-flight mass spectrometry. hIAPP, expected 3903.6, observed 3904.6; rIAPP, expected 3921.3, observed 3921.6; PM, expected 3949.4, observed 3949.2; H18R PM, expected 3969.4, observed 3967.1; F23L PM, expected 3916.4, observed 3915.4. G24P, I26P-IAPP expected 3927.3, observed 3926.7.

Sample Preparation

1.6mM Stock solutions of each peptide were prepared in 100% hexafluoroisopropanol (HFIP). Stock solutions were filtered using 0.45 μM Acrodisc syringe filter with a GHP membrane and the required amount was lyophilized overnight to remove HFIP. Dry peptide was then dissolved into Tris-buffer for the fluorescence assays.

Fluorescence Assays

The kinetics of amyloid formation were monitored using thioflavin-T binding assays conducted with no cosolvent and no stirring at 25°C. Fluorescence measurements were performed using a Beckman Coulter DTX 880 plate reader with a multimode detector using an excitation wavelength of 430 nm and an emission wavelength of 485 nm. Solutions were prepared by dissolving dry peptide into Tris-HCl buffer and thioflavin-T solution immediately before the measurement. The final concentrations were 16 μM hIAPP, 32 μM thioflavin-T in 20 mM Tris-HCl (pH 7.4) with various amounts of the inhibitors.

Transmission Electron Microscopy (TEM)

TEM images were collected at the Life Science Microscopy Center at the State University of New York at Stony Brook. 15 μL aliquots of the samples used for the kinetic studies were removed at the end of each experiment, blotted on a carbon-coated 300-mesh copper grid for 1 min and then negatively stained with saturated uranyl acetate for 1 min.

Mass Spectroscopy Experiments

Peptides were incubated in 20 mM Tris-HCl buffer at pH 7.4. Samples of 1 to 1 mixtures were incubated for 7 days. Samples of 1 to 10 mixtures and controls were incubated for 15 days. Samples were then centrifuged at 17,500g for 45 min. Pellets were collected and rinsed with DDI water twice. After each rinse, samples in DDI water were centrifuged at 17500g for 30 min. The final pellets were depolymerized in 100% (v/v) HFIP and then lyophilized for 20 hours. The peptide samples were analyzed by LC-MS-UV using an Agilent 1260 HPLC and an Agilent G6224A TOF mass spectrometer. The HPLC method uses a Kinetex C18 column; 100Å, 2.6μm, 100×2.1mm, (Phenomenex) at 35°C and 0.55mℓ/min. The HPLC solvents were A: H_2O (0.05% Acetic Acid, 0.05% TFA) and B: CH_3CN (0.05% Acetic Acid, 0.05% TFA). The HPLC solvent gradient method consisted of the following: t=0-1′, B=10%; t=1-5′, B=10-30%; t=5-45′, B=30-50%; t=45-52′, B=50-95%. The ionization source was electrospray ionization in the positive mode. Mass spectra were acquired in the range m/z = 300-3200 with internal calibration using 4 standards. UV chromatograms were acquired at 220and 280nm with a diode array detector.

The ESI positive mass chromatograms were integrated and averaged mass spectra were acquired from the integrated peaks with background subtraction. The mass spectra of the

target peptides were observed in predominantly the +3 and +4 charge states. The resolution of the mass spectrometer in these experiments and in this m/*z* range is ∼13,000. This resolution allows the isotopic distribution of the peptide m/*z* peaks in these charge states to be fully resolved. These mass spectra were deconvoluted using the Agilent resolved isotope deconvolution algorithm, and monoisotopic neutral masses of the peptides were determined with an accuracy of 20 ppm.

Results and Discussion

Pramlintide has a larger effect on the time course of amyloid formation than rIAPP, but co-aggregates with hIAPP

The ability of rIAPP and PM to inhibit amyloid formation by hIAPP were compared using thioflavin-T fluorescence assays and transmission electron microscopy (TEM). Thioflavin-T is a dye whose quantum yield increases upon binding to amyloid fibrils, and it provides a convenient probe of amyloid formation. Thioflavin-T is an extrinsic probe of amyloid formation and the assay can lead to both false positives and negatives, however the dye does not perturb the kinetics of hIAPP amyloid formation under the conditions used here. We first tested mixtures of hIAPP and rIAPP. The kinetic curves measured at different ratios of the two peptides are shown in figure 2. The X-axis is presented as reduced time; time divided by T_{50} of hIAPP, where T_{50} is the time required to reach half of the maximum fluorescence intensity in the assay. No increase in fluorescence intensity of a sample of pure rIAPP was detected during the time course of the experiment, in agreement with a large body of work that has shown that r-IAPP is not amyloidogenic. rIAPP inhibits amyloid formation by hIAPP in a dose dependent manner, consistent with prior studies that made use of a mixed (98%) water, (2%) HFIP solvent system.[20] At low ratios of rIAPP to hIAPP, rIAPP shows a slight inhibitory effect on amyloid formation by hIAPP in buffer, in agreement with the earlier studies.[20] In the present case, T_{50} was increased by a factor of only 1.2 for a 1 to 1 ratio and by a factor of 1.4 for a 1 to 2 ratio (rIAPP is in 2 fold excess). When the concentration of rIAPP was increased to a 5 fold excess, a larger effect was observed as indicated by a 2.2 fold longer T_{50}. This parameter increased by a factor of 3.5 when rIAPP was in 10 fold excess relative to hIAPP. A decrease in the final fluorescence was observed as the concentration of rIAPP was increased. Changes in thioflavin-T intensity are hard to interpret because they can arise from fewer fibrils being formed, or because of the formation of fibrils with reduced capacity to bind thioflavin-T, a change in the degree of association of fibrils, or due to a lower quantum yield of the bound thioflavin-T. Since the fluorescence signal comes from fibril bound thioflavin-T, instead of an intrinsic probe of the fibrils, the values are dependent on how much dye binds and its quantum yield when bound, and this can sometimes give misleading results. Therefore, we collected TEM images at the end of each kinetic experiment. As shown in Figure 3 and Figure S1, TEM confirmed that rIAPP does not aggregate during the time course of the experiment. Images of mixtures of hIAPP and rIAPP showed changes in the amount of fibrils detected on the TEM grid as the concentration of rIAPP increased. At a 1 to 1 ratio, fibrils with typical hIAPP amyloid morphology were observed, and there were no obvious differences in the amount of fibrils detected on the TEM grids of the pure hIAPP sample and the 1:1 sample of hIAPP and rIAPP (figure 3A-B). The 1:2 mixture of hIAPP and rIAPP look similar to the 1:1 samples

and to the sample of pure hIAPP (figure 3D). When the ratio of rIAPP is increased to a 5-fold excess, less extensive mats of fibrils are observed on the TEM grids (figure 3F). The amount of detectable fibrils is noticeably less when the ratio of rIAPP is further increased to a 10-fold excess (figure 3H). It is difficult to detect small differences in fibril morphology by TEM, given the resolution of the method and the negative stains which are employed, but examination of the TEM grids argues that the addition of rIAPP does not perturb the morphology of the individual fibrils.

Two dimensional infrared studies (2DIR) studies conducted at much higher concentrations of rIAPP and hIAPP have shown that rIAPP leads to changes in the structure of hIAPP fibrils.[36] The data presented here shows that rIAPP increases the T_{50} of hIAPP amyloid formation in a dose dependent manner, and also reduces the amount of amyloid fibrils. Our results are consistent with the earlier studies that were conducted in buffers which contained 2% HFIP, and confirm that the behavior of rIAPP is not a consequence of the presence of the organic cosolvent.[20]

We next tested the effect of PM using this assay. PM did not form amyloid during the time course of the study under the conditions used, as indicated by a flat fluorescence curve (figure 2) and TEM (figure S1). Inhibition of hIAPP amyloid formation was observed at all ratios of PM and hIAPP tested and the inhibition effects were dose dependent. PM is more effective at inhibiting the aggregation of hIAPP than rIAPP. An equimolar amount of PM increased T_{50} of hIAPP amyloid formation by a factor of 1.9, compared to the more modest factor of 1.2 observed for rIAPP. T_{50} was further increased to a factor of 2.7 when PM was in 2 fold excess and to 3.9 when PM was in 5 fold excess. When the ratio of hIAPP to PM was 1 to 10, the T_{50} of hIAPP amyloid formation was increased by 5.6 fold. For comparison, rIAPP increased T_{50} by a factor of 3.5 at this ratio.

The final fluorescence intensity of the PM hIAPP mixtures did not change significantly, even in the presence of 10 fold excess of PM. In contrast, a 10-fold excess of rIAPP lead to a decrease in final fluorescence intensity. The fibrils formed at all ratios of PM to hIAPP showed typical IAPP amyloid fibril structure, and there was no detectable reduction in the amount of fibrils on the TEM grid, in contrast to the significant effects on fibril production detected upon the addition of rIAPP (Figure 3). The fibrils formed in the presence of PM appeared to be somewhat thicker than those formed in the presence of rIAPP by visual inspection. Whether this is due to a change in fibril morphology or a difference in the lateral association of fibrils, or simply reflects the staining effects is difficult to judge. However, we believe the key observation is that fewer fibrils are detected in the presence of rIAPP compared to PM, and that PM co-aggregates with hIAP. These results demonstrate that PM is more efficient than rIAPP at inhibiting amyloid formation by hIAPP in terms of the kinetics, but, in contrast to rIAPP, does not cause any detectable change in the amount of fibrils on the TEM grids.

hIAPP induces aggregation of pramlintide

To test if rIAPP or PM were incorporated into the fibrils formed by mixtures of rIAPP or PM with hIAPP under these conditions, we used mass spectrometry. We centrifuged the aggregates formed by mixtures of rIAPP or PM with hIAPP and identified the peptides in

the pellets by redissolving them and conducting LC-MS studies. Control experiments were conducted, in which samples of pure hIAPP, pure rIAPP and pure PM were incubated. A much stronger peak was observed from the pellet formed in the hIAPP control experiments than from the PM or rIAPP control studies, consistent with the fact that hIAPP forms amyloid during the time course of the experiments while the other two peptides do not (Figure S2). Weak peaks were detected for PM and rIAPP which are probably due to residual supernatant in the "pelleted" samples. For the 1 to 1 mixtures of hIAPP with the peptides, we observed only weak peaks due to PM and rIAPP from the pellets, and these had intensities similar to that observed in the control experiments, indicating that neither PM nor rIAPP were significantly incorporated into the fibrils and that the observed fibrils were mainly made up of hIAPP. Similar effects were observed when rIAPP was in 10-fold excess, only a weak peak due to rIAPP was detected from the pellet formed by the mixture of rIAPP and hIAPP, indicating that rIAPP was not incorporated into the pellet under these conditions. Very different results were obtained when PM was added in 10-fold excess. In this case, a strong peak was observed for PM in the pellet formed by the hIAPP PM mixture. The PM peak had a similar intensity to the hIAPP peak in this case (figure 4). There are several possible explanations for this result. hIAPP and PM might co-aggregate into mixed fibrils and thus both be found in the pellet. Alternatively, the two might independently aggregate (either as amyloid or other aggregates) and be sedimented into a pellet. The fact that samples of pure PM do not show appreciable pelletable material argues against this scenario, but does not formally rule out situations where human fibrils promote aggregation of PM into deposits that are largely composed of PM. However, seeding experiments show that hIAPP fibrils do not seed amyloid formation by PM under the conditions of these studies, arguing that it is unlikely that hIAPP fibrils directly promote formation of independent PM fibrils under these conditions (Figure S3).

Mutations of pramlintide make its behavior more like rIAPP

We next examined two point mutants of PM, chosen to make their sequences more rIAPP-like, in order to study the contribution of these sites to the difference in the ability of rIAPP and PM to inhibit hIAPP amyloid formation. There are three differences between rIAPP and hIAPP, in addition to the three prolines. His-18 and Phe-23 in hIAPP are replaced by Arg and Leu respectively in rIAPP (Figure 1). These are less conservative changes than the third substitution which is an Ile-26 to Val mutation. We focused on the least conservative replacements, H18R and F23L. Arg is protonated and charged at pH 7.4 while His is largely deprotonated, thus a H18R replacement changes the charge distribution of the peptide. Electrostatic interactions play an important role in amyloid formation,[37] and hIAPP amyloid formation is pH dependent due to H18 and the free N-terminus.[38-40] The F23L substitution replaces an aromatic residue with an aliphatic side chain and this substitution has been shown to increase the lag time of hIAPP by a factor of two.[41] In contrast, the Ile to Val substitution is more conservative, replacing one β-branched hydrophobic amino acid with another. This substitution leads to a small reduction in hydrophobicity, but maintains a high intrinsic β-sheet propensity at this site. The effect of these point mutations on PM has not been considered, although Green et al have studied the effect of substituting residues from hIAPP into rIAPP using variants with a free C-termini. The derivative of PM with a free c-terminus, denoted here as PM*, was reported to be more amyloidogenic than F23L or H18R

PM* mutants .[42] The naturally occurring polypeptide has an amidated c-terminus and variants without this modification have been shown to behave differently than the physiologically relevant amidated form and to have altered amyloidogenicity, none-the-less the results are consistent with the notion that a higher sequence similarity to the human peptide leads to higher amyloidogenic potential.[39, 43]

The kinetics of amyloid formation by mixtures of hIAPP with each of these mutants are depicted in figure 5. Pure samples of H18R PM and F23L PM did not form amyloid during the time course of the study, as indicated by their flat fluorescence time courses and by TEM (Figure 5, Figure 6 and Figure 7). Dose dependent inhibition effects were observed for both mutants. Both of the mutants behaved more like rIAPP than PM, in the sense that they were less effective inhibitors than PM. The inhibitory effects of H18R PM and F23L PM were almost the same in terms of their effects on the value of T_{50} (Figure 8). As the concentration of peptide was increased, H18R PM showed a more obvious effect on the final thioflavin-T fluorescence intensity than did F23L PM (Figure 5). However, all of the TEM images collected of mixtures of either mutant with hIAPP at different ratios showed typical amyloid fibril structure. Extensive mats of fibrils were observed, and in this sense they behaved more like PM than like rIAPP (Figure 6, Figure 7).

Conclusions

The effect of the four peptide inhibitors on the value of T_{50} for hIAPP amyloid formation are summarized in figure 8. Our results show that PM is more efficient than rIAPP in inhibiting amyloid formation by hIAPP, however, in contrast to rIAPP, it does not affect the amount of fibrils detectable by TEM. The mass spectroscopy analysis of the amyloid fibrils formed by mixtures of PM with hIAPP and rIAPP with hIAPP argue that PM interacts more strongly with hIAPP than rIAPP does under the condition of these experiments, and is either incorporated into the amyloid fibers or induced to co-aggregate.

These results argue that, all else being equal, a higher sequence similarity to hIAPP leads to a non-amyloidgenic mutant being a better inhibitor of hIAPP amyloid formation provided a strong β-breaker element is retained, likely due to more efficient sequence recognition. rIAPP and the two mutants of PM, H18R PM and F23L PM, are less effective inhibitors than PM, consistent with this hypothesis, however, the correlation is not perfect since the two PM single mutants do not outperform rIAPP even though they have a higher sequence identity to hIAPP. The helical recognition models argues that residue-18 plays a role in initial contacts and more recent work implicates residues near position 23 in the early stages of hIAPP amyloid formation.[31] It may be that converting just one of these positions from the human residue is enough to induce a significant effect and to render the PM peptide more “rat-like” in its behavior.

Based on a set of elegant experiments, Middleton et al have constructed a detailed model of how rIAPP inhibits hIAPP amyloid formation. Isotope edited two-dimensional infrared and TEM studies were conducted under different conditions than employed here. In those studies, both peptides were present at much higher concentrations, required to ensure sufficient signal to noise in the IR studies. Under these conditions rIAPP first blocks the

formation of the C-terminal β-sheet, thereby explaining the increased lag time. rIAPP then loses this effect and the recognition sequence in rIAPP forms its own β-sheet rich aggregates.[36] The resolution of the methods employed here do not allow one to determine if PM forms its own fibrils or is incorporated into the hIAPP fibrils, but the LC-MS studies indicate that rIAPP is not incorporated into the fibrils under the conditions of our studies, where it is present at much lower concentrations than in the IR experiments. It is important to note that there is no inconsistency between this study and the earlier work since they were conducted under significantly different conditions and aggregation is expected to be much more facile at higher peptide concentrations.

The comparison of rIAPP and PM argues that peptide based inhibitor design involves a trade-off between more efficient recognition of the target protein and the higher amyloidogenicity attributed to higher sequence similarity. An optimum balance should lead to the best inhibition efficiency, for a given set of peptides. Having too low a sequence identity may prevent the peptide from effectively interacting with the target peptide, while having too high a similarity may lead to mixed aggregates formed by the designed inhibitor and the target peptide. PM appears to be balanced between these effects. This does not mean that PM is the optimum peptide based inhibitor. Other variants of hIAPP, that use fewer proline residues and target different sites, have larger effects on hIAPP amyloid formation, likely because the other sites are more important for β-sheet formation and because the use of fewer proline substitutions can lead to better recognition.[17, 18]

Data sets from a G24P, I26P double proline mutant of hIAPP (DM-IAPP) support the notation of a trade-off between recognition and β-sheet inhibition. We have previously shown that each of the single mutants is an inhibitor of amyloid formation by wild type hIAPP.[17, 44] Each is more effective than rIAPP or PM. Here we show that the double mutant is also an inhibitor, but is much less effective than the single mutant. (Figure S4). In this case, the single site mutations are sufficient to reduce amyloidogenicity, and the higher sequence identity presumably leads to better recognition of the human sequence and more effective inhibitors. The fact that the double proline mutant is a less effective inhibitor of hIAPP amyloid formation than either of the single mutants suggests that they interact with hIAPP in a more complicated manner than simply through the region with the major helical propensity since they are identical in this segment.[45] Along these lines, the two substitutions are located within a region of hIAPP that has been identified by 2DIR spectroscopy as being of importance in the early steps in hIAPP amyloid formation.[31] The 2DIR studies indicate that transient β-sheet structure is formed in this region during amyloid formation by hIAPP. It is also interesting to note that the double proline mutant is a noticeably less effective inhibitor than a variant of hIAPP that contain N-methylated residues at positions 24 and 26.[18] A double Gly, Ile to Pro mutation is a much larger change than replacing Gly and Ile with N-methyl Gly and N-methyl Leu and should be more perturbing to inhibitor hIAPP interactions. In this case, it appears that the N-methylated variant is close to optimal.

Supplementary Material

Refer to Web version on PubMed Central for supplementary material.

Acknowledgments

Funding Sources: This work was supported by a grant from the United States National Institutes of Health, GM078114, to D. P. R. Z.R was supported in part by an NIH training grant 5T32GM09271405

We thank Dr. Andisheh Abedini and Dr Fangling Meng for preliminary studies with the G24P,I26P double mutant and Dr. Abedini and Prof. Martin Zanni for numerous helpful discussions.

References

1. Sipe JD. Amyloidosis. Crit Rev Clin Lab Sci. 1994; 31:325–354. [PubMed: 7888076]
2. Vendruscolo M, Zurdo J, MacPhee CE, Dobson CM. Protein folding and misfolding: a paradigm of self-assembly and regulation in complex biological systems. Philos Trans A Math Phys Eng Sci. 2003; 361:1205–1222. [PubMed: 12816607]
3. Cooper GJ, Willis AC, Clark A, Turner RC, Sim RB, Reid KB. Purification and characterization of a peptide from amyloid-rich pancreases of type 2 diabetic patients. Proc Natl Acad Sci. 1987; 84:8628–8632. [PubMed: 3317417]
4. Westermark P, Wernstedt C, O'Brien TD, Hayden DW, Johnson KH. Islet amyloid in type 2 human diabetes mellitus and adult diabetic cats contains a novel putative polypeptide hormone. Am J Pathol. 1987; 127:414–417. [PubMed: 3296768]
5. Clark A, Wells CA, Buley ID, Cruickshank JK, Vanhegan RI, Matthews DR, Cooper GJ, Holman RR, Turner RC. Islet amyloid, increased A-cells, reduced B-cells and exocrine fibrosis: quantitative changes in the pancreas in type 2 diabetes. Diabetes Res Clin Pract. 1988; 9:151–159.
6. Westermark P, Grimeliu L. Pancreatic-islet cells in insular amyloidosis in human diabetic and non-diabetic adults. Acta Pathol Microbiol Scand. 1973; A 81:291–300.
7. Westermark P, Wilander E. The influence of amyloid deposits on the islet volume in maturity onset diabetes mellitus. Diabetologia. 1978; 15:417–421. [PubMed: 367856]
8. Andersson A, Bohman S, Borg LA, Paulsson JF, Schultz SW, Westermark GT, Westermark P. Amyloid deposition in transplanted human pancreatic islets: a conceivable cause of their long-term failure. Exp Diabetes Res. 2008; 2008:562985. [PubMed: 19277203]
9. Potter KJ, Abedini A, Marek P, Klimek AM, Butterworth S, Driscoll M, Baker R, Nilsson MR, Warnock GL, Oberholzer J, Bertera S, Trucco M, Korbutt GS, Fraser PE, Raleigh DP, Verchere CB. Islet amyloid deposition limits the viability of human islet grafts but not porcine islet grafts. Proc Natl Acad Sci USA. 2010; 107:4305–4310. [PubMed: 20160085]
10. Porat Y, Mazor Y, Efrat S, Gazit E. Inhibition of islet amyloid polypeptide fibril formation: A potential role for heteroaromatic interactions. Biochemistry. 2004; 43:14454–14462. [PubMed: 15533050]
11. Mishra R, Sellin D, Radovan D, Gohlke A, Winter R. Inhibiting islet amyloid polypeptide fibril formation by the red wine compound resveratrol. ChemBioChem. 2009; 10:445–449. [PubMed: 19165839]
12. Kapurniotu A, Schmauder A, Tenidis K. Structure-based design and study of non-amyloidogenic, double N-methylated IAPP amyloid core sequences as inhibitors of IAPP amyloid formation and cytotoxicity. J Mol Biol. 2002; 315:339–350. [PubMed: 11786016]
13. Porat Y, Abramowitz A, Gazit E. Inhibition of amyloid fibril formation by polyphenols: structural similarity and aromatic interactions as a common inhibition mechanism. Chemical Biology & Drug Design. 2006; 67:27–37. [PubMed: 16492146]
14. Young LM, Cao P, Raleigh DP, Ashcroft AE, Radford SE. Ion mobility spectrometry–mass spectrometry defines the oligomeric intermediates in amylin amyloid formation and the mode of action of inhibitors. J Am Chem Soc. 2013; 136:660–670. [PubMed: 24372466]
15. Noor H, Cao P, Raleigh DP. Morin hydrate inhibits amyloid formation by islet amyloid polypeptide and disaggregates amyloid fibers. Protein Sci. 2012; 21:373–382. [PubMed: 22238175]
16. Cao P, Raleigh DP. Analysis of the inhibition and remodeling of islet amyloid polypeptide amyloid fibers by flavanols. Biochemistry. 2012; 51:2670–2683. [PubMed: 22409724]

17. Meng FL, Raleigh DP, Abedini A. Combination of kinetically selected Inhibitors in trans leads to highly effective inhibition of amyloid formation. J Am Chem Soc. 2010; 132:14340–14342. [PubMed: 20873820]
18. Yan LM, Tatarek-Nossol M, Velkova A, Kazantzis A, Kapurniotu A. Design of a mimic of nonamyloidogenic and bioactive human islet amyloid polypeptide (IAPP) as nanomolar affinity inhibitor of IAPP cytotoxic fibrillogenesis. Proc Natl Acad Sci U S A. 2006; 103:2046–2051. [PubMed: 16467158]
19. Lorenzo A, Razzaboni B, Weir GC, Yankner BA. Pancreatic islet cell toxicity of amylin associated with type-2 diabetes mellitus. Nature. 1994; 368:756–760. [PubMed: 8152488]
20. Cao P, Meng F, Abedini A, Raleigh DP. The ability of rodent islet amyloid polypeptide to inhibit amyloid formation by human islet amyloid polypeptide has important implications for the mechanism of amyloid formation and the design of inhibitors. Biochemistry. 2010; 49:872–881. [PubMed: 20028124]
21. Westermark P, Engstrom U, Johnson KH, Westermark GT, Betsholtz C. Islet amyloid polypeptide: pinpointing amino acid residues linked to amyloid fibril formation. Proc Natl Acad Sci U S A. 1990; 87:5036–5040. [PubMed: 2195544]
22. Gedulin BR, Rink TJ, Young AA. Dose-response for glucagonostatic effect of amylin in rats. Metabolism. 1997; 46:67–70. [PubMed: 9005972]
23. Samsom M, Szarka LA, Camilleri M, Vella A, Zinsmeister AR, Rizza RA. Pramlintide, an amylin analog, selectively delays gastric emptying: potential role of vagal inhibition. Am J Physiol Gastrointest Liver Physiol. 2000; 278:G946–951. [PubMed: 10859225]
24. Hebda JA, Miranker AD. The Interplay of Catalysis and Toxicity by Amyloid Intermediates on Lipid Bilayers: Insights from Type II Diabetes. Ann Rev Biophys. 2009; 38:125–152. [PubMed: 19416063]
25. Rushing PA, Hagan MM, Seeley RJ, Lutz TA, D'Alessio DA, Air EL, Woods SC. Inhibition of central amylin signaling increases food intake and body adiposity in rats. Endocrinology. 2001; 142:5035–5038. [PubMed: 11606473]
26. Clementi G, Caruso A, Cutuli VMC, deBernardis E, Prato A, AmicoRoxas M. Amylin given by central or peripheral routes decreases gastric emptying and intestinal transit in the rat. Experientia. 1996; 52:677–679. [PubMed: 8698109]
27. Kruger DF, Gloster MA. Pramlintide for the treatment of insulin-requiring diabetes mellitus - Rationale and review of clinical data. Drugs. 2004; 64:1419–1432. [PubMed: 15212559]
28. Mazor Y, Gilead S, Benhar I, Gazit E. Identification and Characterization of a Novel Molecular-recognition and Self-assembly Domain within the Islet Amyloid Polypeptide. J Mol Biol. 2002; 322:1013–1024. [PubMed: 12367525]
29. Wiltzius JJW, Sievers SA, Sawaya MR, Eisenberg D. Atomic structures of IAPP (amylin) fusions suggest a mechanism for fibrillation and the role of insulin in the process. Protein Sci. 2009; 18:1521–1530. [PubMed: 19475663]
30. Dupuis NF, Wu C, Shea JE, Bowers MT. The Amyloid Formation Mechanism in Human IAPP: Dimers Have β-Strand Monomer—Monomer Interfaces. J Am Chem Soc. 2011; 133:7240–7243. [PubMed: 21517093]
31. Buchanan LE, Dunkelberger EB, Tran HQ, Cheng PN, Chiu CC, Cao P, Raleigh DP, de Pablo JJ, Nowick JS, Zanni MT. Mechanism of IAPP amyloid fibril formation involves an intermediate with a transient beta-sheet. Proc Natl Acad Sci U S A. 2013; 110:19285–19290. [PubMed: 24218609]
32. Nonoyama A, Laurence JS, Garriques L, Qi H, Le T, Middaugh CR. A biophysical characterization of the peptide drug pramlintide (AC137) using empirical phase diagrams. J Pharm Sci. 2008; 97:2552–2567. [PubMed: 17879973]
33. Abedini A, Raleigh DP. Incorporation of pseudoproline derivatives allows the facile synthesis of human IAPP, a highly amyloidogenic and aggregation-prone polypeptide. Org Lett. 2005; 7:693–696. [PubMed: 15704927]
34. Marek P, Woys AM, Sutton K, Zanni MT, Raleigh DP. Efficient microwave-assisted synthesis of human islet amyloid polypeptide designed to facilitate the specific incorporation of labeled amino acids. Org Lett. 2010; 12:4848–4851. [PubMed: 20931985]

35. Abedini A, Singh G, Raleigh DP. Recovery and purification of highly aggregation-prone disulfide-containing peptides: Application to islet amyloid polypeptide. Anal Biochem. 2006; 351:181–186. [PubMed: 16406209]
36. Middleton CT, Marek P, Cao P, Chiu CC, Singh S, Woys AM, de Pablo JJ, Raleigh DP, Zanni MT. Two-dimensional infrared spectroscopy reveals the complex behaviour of an amyloid fibril inhibitor. Nat Chem. 2012; 4:355–360. [PubMed: 22522254]
37. Marek PJ, Patsalo V, Green DF, Raleigh DP. Ionic strength effects on amyloid formation by amylin are a complicated interplay among Debye screening, ion selectivity, and Hofmeister effects. Biochemistry. 2012; 51:8478–8490. [PubMed: 23016872]
38. Abedini A, Raleigh DP. The role of His-18 in amyloid formation by human islet amyloid polypeptide. Biochemistry. 2005; 44:16284–16291. [PubMed: 16331989]
39. Tu LH, Serrano Arnaldo L, Zanni Martin T, Raleigh Daniel P. Mutational analysis of preamyloid intermediates: The role of His-Tyr interactions in islet amyloid formation. Biophys J. 2014; 106:1520–1527. [PubMed: 24703313]
40. Jha S, Snell JM, Sheftic SR, Patil SM, Daniels SB, Kolling FW, Alexandrescu AT. pH dependence of amylin fibrillization. Biochemistry. 2013; 53:300–310. [PubMed: 24377660]
41. Tu LH, Raleigh DP. Role of Aromatic Interactions in Amyloid Formation by Islet Amyloid Polypeptide. Biochemistry. 2013; 52:333–342. [PubMed: 23256729]
42. Green J, Goldsbury C, Mini T, Sunderji S, Frey P, Kistler J, Cooper G, Aebi U. Full-length Rat Amylin Forms Fibrils Following Substitution of Single Residues from Human Amylin. J Mol Biol. 2003; 326:1147–1156. [PubMed: 12589759]
43. Chen MS, Zhao DS, Yu YP, Li WW, Chen YX, Zhao YF, Li YM. Characterizing the assembly behaviors of human amylin: a perspective derived from C-terminal variants. Chem Commun. 2013; 49:1799–1801.
44. Abedini A, Meng FL, Raleigh DP. A single-point mutation converts the highly amyloidogenic human islet amyloid polypeptide into a potent fibrillization inhibitor. J Am Chem Soc. 2007; 129:11300–11301. [PubMed: 17722920]
45. Williamson JA, Miranker AD. Direct detection of transient alpha-helical states in islet amyloid polypeptide. Protein Sci. 2007; 16:110–117. [PubMed: 17123962]

Abbreviations

hIAPP	human islet amyloid polypeptide
rIAPP	rat islet amyloid polypeptide
DM-IAPP	double mutant islet amyloid polypeptide
PM	pramlintide
PM*	pramlintide with free C-terminus
T2D	type II dibates
TFA	trifluoroacetic acid
HFIP	hexafluoroisopropanol

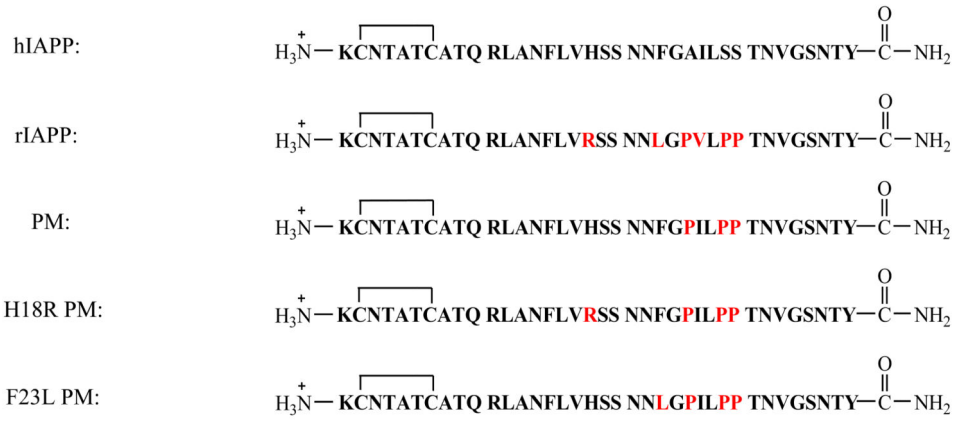

Figure 1.

Sequence of hIAPP, rIAPP, PM, H18R PM and F23L PM. Each peptide contains a disulfide bond connecting Cys 2 and Cys 7 and has an amidated C-terminus. Residues which differ from hIAPP are colored red.

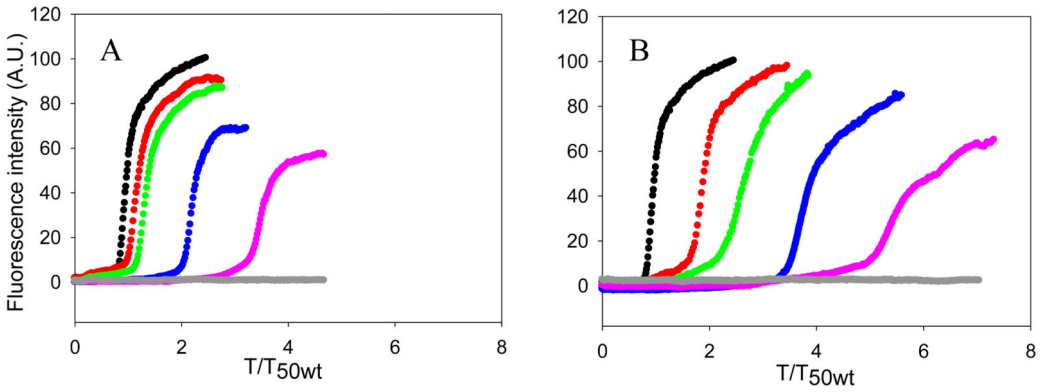

Figure 2.

Pramlintide (PM) is a more effective inhibitor of amyloid formation by wild type hIAPP than is rIAPP. (A) The kinetics of hIAPP amyloid formation in the presence of rIAPP monitored by thioflavin-T fluorescence assays. Black, hIAPP; red, a 1:1 mixture of hIAPP and rIAPP; green, a mixture of hIAPP and rIAPP at a 1 to 2 ratio; blue, a mixture of hIAPP and rIAPP at a 1 to 5 ratio; pink, a mixture of hIAPP and rIAPP at a 1 to 10 ratio; grey, 160 μM rIAPP. (B) The kinetics of hIAPP amyloid formation in the presence of PM monitored by thioflavin-T fluorescence essays. The same color coding is used as in panel A. Experiments were conducted in 20 mM Tris-HCl (pH 7.4), without stirring at 25 °C. The concentration of hIAPP was 16 μM.

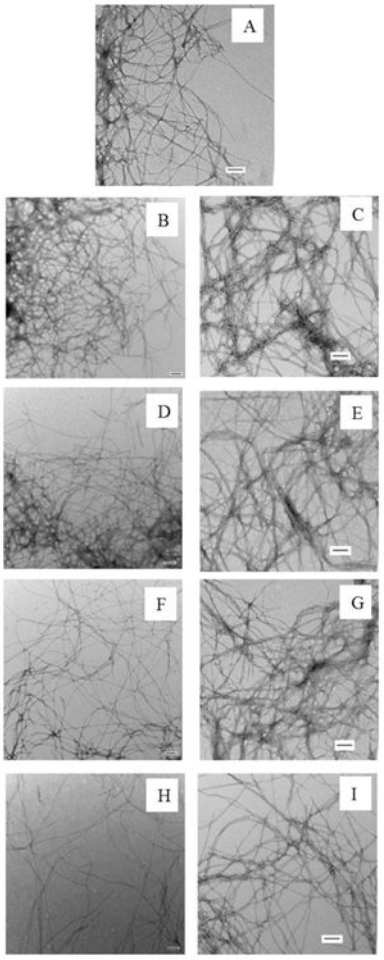

Figure 3.

Comparison of the final products of the experiments shown in Figure 2. (A) TEM image of hIAPP. (B) TEM image of a 1:1 mixture of hIAPP and rIAPP. (C) TEM image of a 1:1 mixture of hIAPP and PM. (D) TEM image of a 1:2 mixture of hIAPP and rIAPP. (E) TEM image of a 1:2 mixture of hIAPP and PM. (F) TEM image of a 1:5 mixture of hIAPP and rIAPP. (G) TEM image of a 1:5 mixture of hIAPP and PM. (H) TEM image of a 1:10 mixture of hIAPP and rIAPP. (I) TEM image of a 1:10 mixture of hIAPP and PM. All images were collected at the end of the kinetic experiments shown in figure 2. Scale bars represent 100 nm.

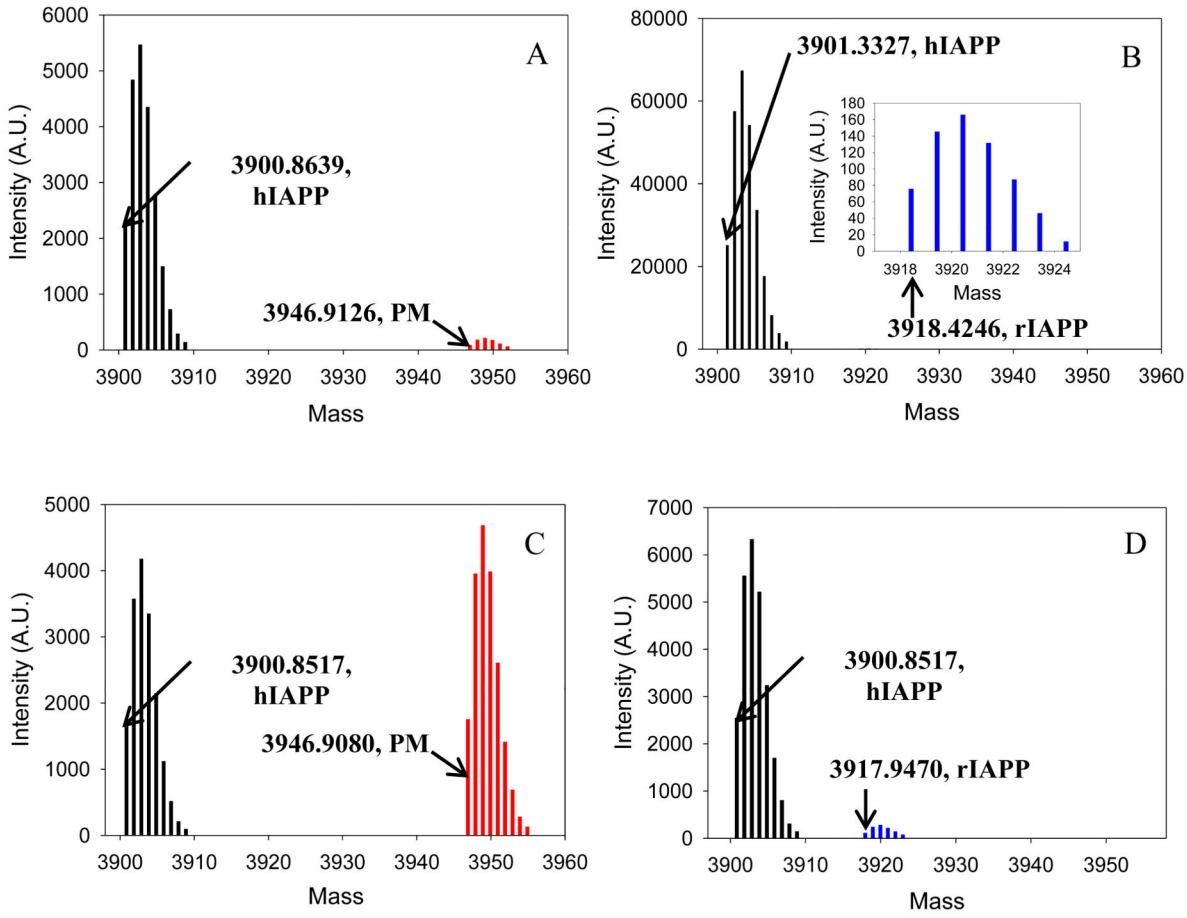

Figure 4.

Results of co-incubation experiments. Samples of a 1 to 1 mixture were incubated for 7 days, and samples of a 1 to 10 mixture were incubated for 15 days in 20 mM Tris-HCl (pH 7.4), without stirring at 25 °C. Each sample was then pelleted, depolymerized, and analyzed by LC-MS. (A) Results of a 1 to 1 mixture of hIAPP and PM. Black, hIAPP; red, PM. (B) Results of a 1 to 1 mixture of hIAPP and rIAPP. Black, hIAPP; blue, rIAPP. The inset is an expansion of the region from 3917 to 3925, and shows the peak due to rIAPP. (C) Results of a 1 to 10 mixture of hIAPP and PM. PM was in 10 fold excess. Black, hIAPP; red, PM. (D) Results of a 1 to 10 mixture of hIAPP and rIAPP. rIAPP was in 10 fold excess. Black, hIAPP; blue, rIAPP. Data shown in this figure are deconvoluted apparent neutral mass.

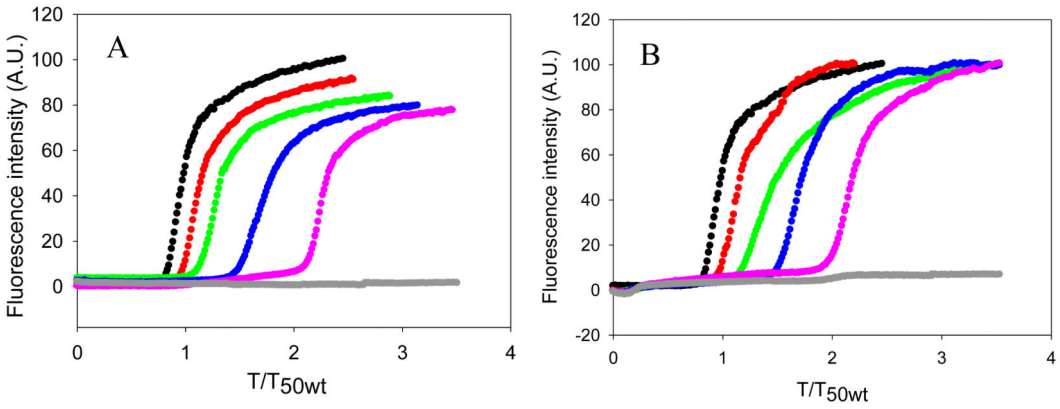

Figure 5.

Effects of replacing His-18 and Phe-23 in PM by the corresponding residues of rIAPP. (A) The kinetics of hIAPP amyloid formation in the presence of H18R PM monitored by thioflavin-T fluorescence assays. Black, hIAPP; red, a 1:1 mixture of hIAPP and H18R PM; green, a mixture of hIAPP and H18R PM at a 1 to 2 ratio; blue, a mixture of hIAPP and H18R PM at a 1 to 5 ratio; pink, a mixture of hIAPP and H18R PM at a 1 to 10 ratio; grey, 160 μM H18R PM. (B) The kinetics of hIAPP amyloid formation in the presence of F23L PM monitored by thioflavin-T fluorescence essays. The same color coding is used here as in panel A. The kinetic experiments were conducted in 20 mM Tris-HCl (pH 7.4), without stirring at 25 °C. The concentration of hIAPP was 16 μM.

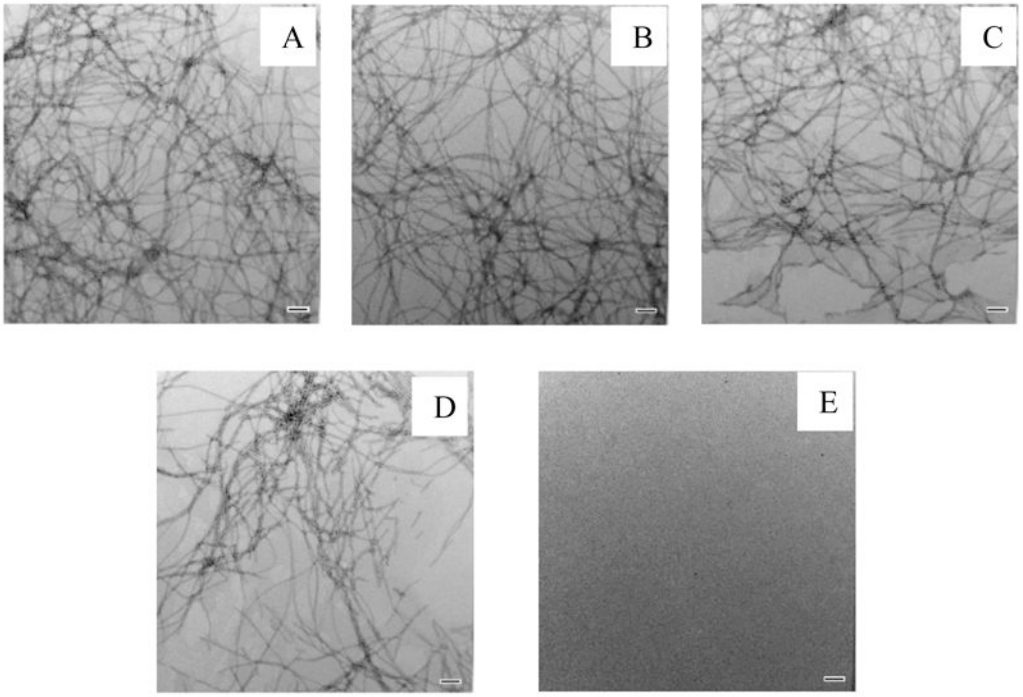

Figure 6.

TEM images of mixtures of hIAPP and H18R PM at different ratios of the two peptides. (A) TEM image of a 1:1 mixture of hIAPP and H18R PM. (B) TEM image of a 1:2 mixture of hIAPP and H18R PM. (C) TEM image of a 1:5 mixture of hIAPP and H18R PM. (D) TEM image of a 1:10 mixture of hIAPP and H18R PM. (E) TEM image of pure H18R PM at 160 μM. Images were collected at the end of the kinetic experiments shown in figure 5A. Scale bars represent 100 nm.

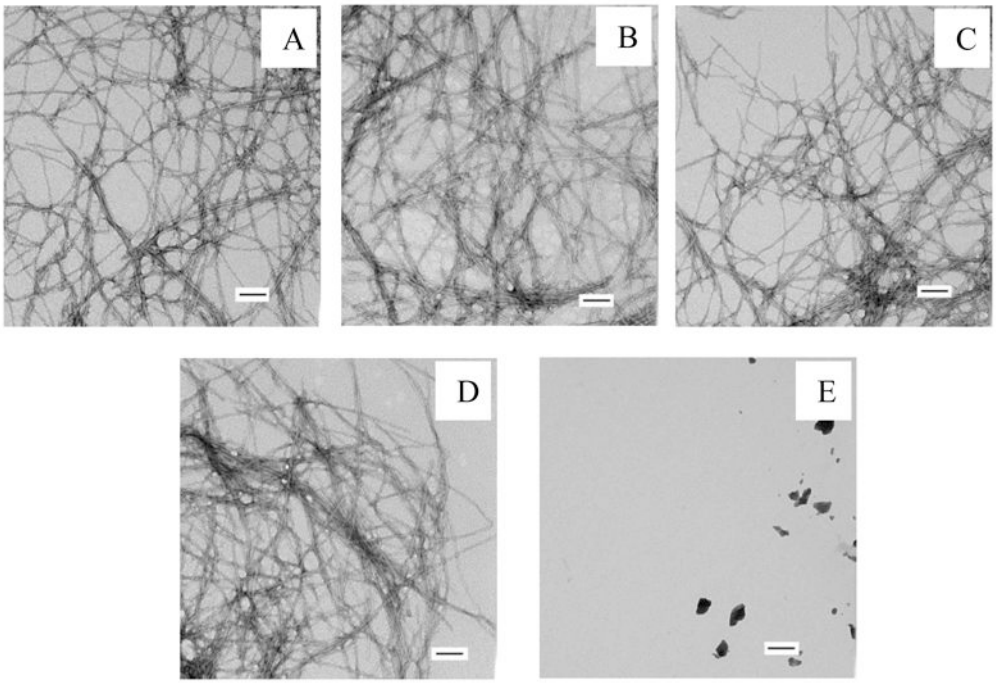

Figure 7.

TEM images of mixtures of hIAPP and F23L PM. (A) TEM image of a 1:1 mixture of hIAPP and F23L PM. (C) TEM image of a 1:2 mixture of hIAPP and F23L PM. (D) TEM image of a 1:5 mixture of hIAPP and F23L PM. (E) TEM image of a 1:10 mixture of hIAPP and F23L PM. (F) TEM image of pure F23L PM at 160 μM. Images were collected at the end of the kinetic experiments shown in figure 5B. Scale bars represent 100 nm.

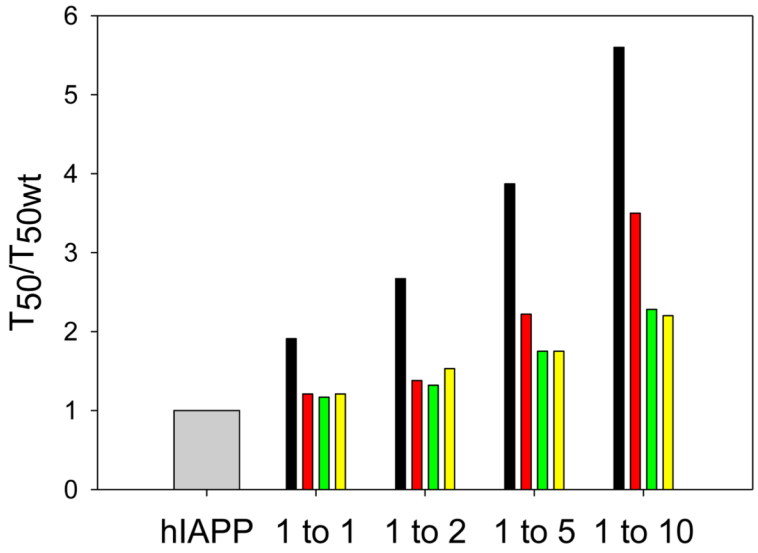

Figure 8.

Summary of the effect of the different inhibitors on amyloid formation by hIAPP. The factors by which the T_{50} for wild type hIAPP amyloid formation was increased are plotted as; grey, hIAPP alone; black, mixtures of hIAPP and PM at different ratios; red, mixtures of hIAPP and rIAPP at different ratios; green, mixtures of hIAPP and H18R PM at different ratios; yellow, mixtures of hIAPP and F23L PM at different ratios. Values were determined from the kinetic curves shown in figure 2 and figure 5.